

УДК 621.315.592

# Valence band structure of binary chalcogenide vitreous semiconductors by high-resolution XPS

© S. Kozyukhin<sup>¶</sup>, R. Golovchak<sup>\*</sup>, A. Kovalskiy<sup>†</sup>, O. Shpotyuk<sup>\*</sup>, H. Jain<sup>†</sup>

Institute of General and Inorganic Chemistry,  
Russian Academy of Science,  
199991 Moscow, Russia

<sup>\*</sup> Lviv Scientific Research Institute of Materials of SRC „Carat“,  
UA-79031 Lviv, Ukraine

<sup>†</sup> Department of Materials Science and Engineering,  
Lehigh University, Bethlehem,  
PA 18015-3195, USA

(Получена 14 сентября 2010 г. Принята к печати 20 сентября 2010 г.)

High-resolution X-ray photoelectron spectroscopy (XPS) is used to study regularities in the formation of valence band electronic structure in binary  $As_xSe_{100-x}$ ,  $As_xS_{100-x}$ ,  $Ge_xSe_{100-x}$  and  $Ge_xS_{100-x}$  chalcogenide vitreous semiconductors. It is shown that the highest occupied energetic states in the valence band of these materials are formed by lone pair electrons of chalcogen atoms, which play dominant role in the formation of valence band electronic structure of chalcogen-rich glasses. A well-expressed contribution from chalcogen bonding  $p$  electrons and more deep  $s$  orbitals are also recorded in the experimental valence band XPS spectra. Compositional dependences of the observed bands are qualitatively analyzed from structural and compositional points of view.

## 1. Introduction

Chalcogenide vitreous semiconductors (ChVS) attracted a substantial attention after discovering of their semi-conducting properties in 1950<sup>th</sup> by B.T. Kolomiets and N.A. Goryunova [1]. However, despite vast expectations the application of ChVS in semiconductor electronics is still limited up to now, mostly because of non-doping ability of bulk ChVS typically having  $p$ -type of conductivity and Fermi level pinned near the middle of band gap [2,3]. Instead, these materials have found other promising applications in optoelectronics and photonics as high efficiency optical amplifiers in optical communication networks, memory or switching devices, high-resolution inorganic photoresists, media for submicrometer lithography process, antireflection coatings, etc [4–7]. These applications became possible owing to considerable last-years efforts of numerous researchers, who have achieved a significant progress in studying of the interrelation between physical-chemical properties of these materials and their atomic structure. On the other hand, the analogous interrelation with electronic structure of ChVS is not so extensively studied. The attention was paid mainly to general features in the valence band of these materials [8–15], while their relation to systematic changes in composition or structural peculiarities of binary glasses is studied insufficiently. Notwithstanding, it is known that any changes in electronic subsystem of ChVS lead to changes in their atomic subsystem, because ChVS belong to the class of materials with strong electron-phonon coupling [2,3,16]. The discovered recently optomechanical effect [17] or physical ageing induced by above-bandgap photoexposure [18] are

only some examples of the effects related to such coupling. Thus, the understanding of main regularities in the formation of ChVS electronic structure will help to develop new optoelectronic functional devices capable to explore atomic and electronic subsystems of ChVS with the same efficiency.

In the present paper, we apply high-resolution X-ray photoelectron spectroscopy (XPS) technique to study regularities in the formation of valence band in typical binary sulfide and selenide ChVS owing to systematic variation of their composition. So far, only a few high-resolution XPS studies have been conducted on selenide and sulfide bulk glasses mostly of stoichiometric compositions [8–15].

## 2. Experimental

The samples of binary  $As_xSe_{100-x}$ ,  $As_xS_{100-x}$ ,  $Ge_xSe_{100-x}$  and  $Ge_xS_{100-x}$  ChVS were prepared by conventional melt quenching route in evacuated quartz ampoules from a mixture of high purity powders using rocking furnace. The amorphous state of the prepared samples was inferred visually by the characteristic conch-like fracture of the specimens, differential scanning calorimetry and X-ray diffraction data.

XPS is a surface analysis technique with about 65% of the signal originating from the outermost  $\sim 30 \text{ \AA}$  of the surface. To obtain data representative of the bulk, glass specimens were fractured inside the analysis chamber at pressures typically  $2 \cdot 10^{-8}$  mbar or less. This procedure eliminated ambiguities that might be introduced into the spectra as a result of surface reactions with oxygen or other contaminations.

The XPS spectra were recorded with a Scienta ESCA-300 spectrometer using monochromatic Al  $K_{\alpha}$  X-ray

<sup>¶</sup> E-mail: sergkoz@igic.ras.ru

(1486.6 eV). The analysis area was a spot  $\sim 3\text{--}4\text{ mm}$  long and  $\sim 250\ \mu\text{m}$  wide. Data acquisition was restricted electronically to a region smaller than the X-ray illuminated area. For all measurements the angle between the surface and the detector was  $90^\circ$ . The instrument was operated in a mode that yielded a Fermi-level width of 0.4 eV for Ag metal and at a full width a half maximum of 0.54 eV for Ag  $3d_{5/2}$  core level peak. Energy scale was calibrated using the Fermi level of clean Ag.

The XPS data consisted of survey scans over the entire binding energy (BE) range (to control the purity of the samples) and scans over the valence bands of the investigated ChVS. The valence band spectra were recorded by sweeping the retarding field and using the constant pass energy of 300 eV. The reproducibility of the measurements was checked on different regions of fractured surfaces as well as on different samples. The surface charging from photoelectron emission was neutralized using a low energy ( $< 10\text{ eV}$ ) electron flood gun. Though effective in minimizing distortions that might arise from differential surface charging on the fracture surfaces, the use of the flood gun resulted in the surfaces attaining a uniform, though net negative potential with respect to earth. The magnitude of this potential depended upon the geometry and conductivity of the surface. The experimental positions of the valence band spectra for all the investigated samples were adjusted by referencing to the  $4f_{7/2}$  core level peak of pure Au at 84.0 eV as described elsewhere [8].

Data analysis was conducted with standard CASA-XPS software package. Intensities of the XPS signals recorded for different samples were normalized to the high-energy background level for comparison.

### 3. Results and discussion

The survey XPS spectra of fractured surfaces have shown only peaks associated with the core levels of constituting elements (As or Ge, S or Se) as well as related Auger lines, which have been identified using the reference spectra in the PHI handbook [19]. No elements other than the glass components were observed in the spectra. In particular, there was no evidence for oxygen in large concentration on any of the surfaces.

Valence band spectra obtained for As-based ChVS are shown in Figs 1 and 2 for selenide and sulfide glasses, respectively. Increase in As concentration ( $x$ ) within the  $\text{As}_x\text{Se}_{100-x}$  or  $\text{As}_x\text{S}_{100-x}$  system leads to a number of characteristic modifications in these spectra. First of all the valley at  $\sim 3\text{ eV}$  disappears due to the broadening of Se  $4p$  or S  $3p$  bonding states peak as the number of Se–As or S–As bonds increases (As  $4p$  bonding states give a peak at this value of binding energy) [8,9]. An accompanying decrease in the band intensity at  $\sim 5\text{ eV}$  is explained by a decrease in the Se  $4p$  or S  $3p$  bonding states associated with Se–Se or S–S covalent bonds [8,10,11]. Smooth changes in the intensity of XPS signal from  $lp$  electrons ( $\sim 2\text{ eV}$ )

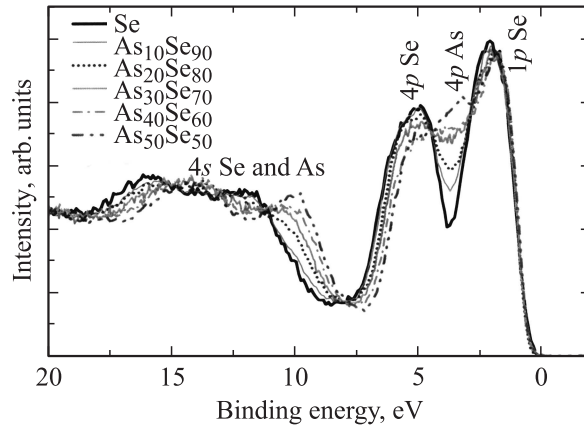


**Fig. 1.** Compositional behavior of XPS valence band spectra for  $\text{As}_x\text{Se}_{100-x}$  glasses.

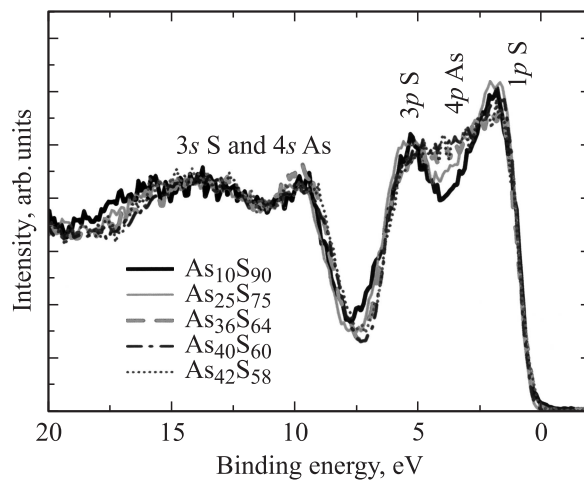


**Fig. 2.** Compositional behavior of XPS valence band spectra for  $\text{As}_x\text{S}_{100-x}$  glasses.

of Se or S (Figs 1, 2) correlate well with the expected compositional behavior: higher the chalcogen content, the stronger is the signal from lone pair  $lp$  electrons because every chalcogen atom contributes by its own  $lp$  electrons. It should be noted also, that full width at half maximum of whole broad feature at  $0\text{--}6\text{ eV}$  decreases with increasing As content in the samples of  $\text{As}_x\text{Se}_{100-x}$  system, while analogous decrease (if any) for  $\text{As}_x\text{S}_{100-x}$  ChVS is remarkably less. Additionally, in the case of  $\text{As}_x\text{Se}_{100-x}$  ChVS (Fig. 1), the broad band at  $9\text{--}16\text{ eV}$  can be decomposed into 4 different regions (centered at 9, 11, 14 and 16 eV), while this tendency is less expressed for  $\text{As}_x\text{S}_{100-x}$  glasses (Fig. 2). Above features originate from interaction of As  $4s$ , Se  $4s$  or S  $3s$  electrons with As  $4p^\sigma$  and chalcogen (Se  $4p^\sigma$  or S  $3p^\sigma$ ) bonding electrons [20].

The compositional behavior of valence band XPS spectra for Ge-based ChVS is shown in Figs 3 and 4 for the investigated selenide and sulfide glasses, respectively. It correlates well with experimental and theoretical data

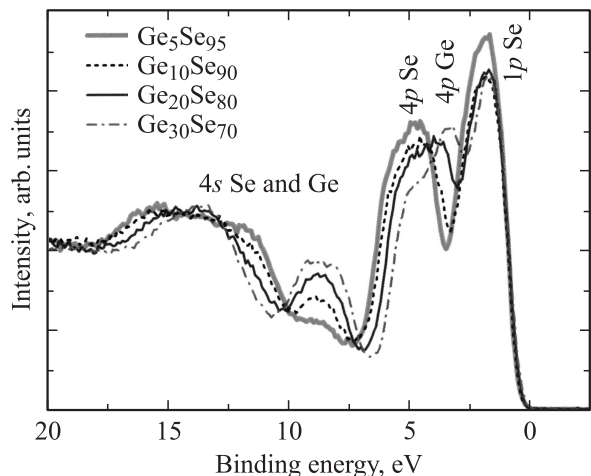


**Fig. 3.** Compositional behavior of XPS valence band spectra for  $\text{Ge}_x\text{Se}_{100-x}$  glasses.

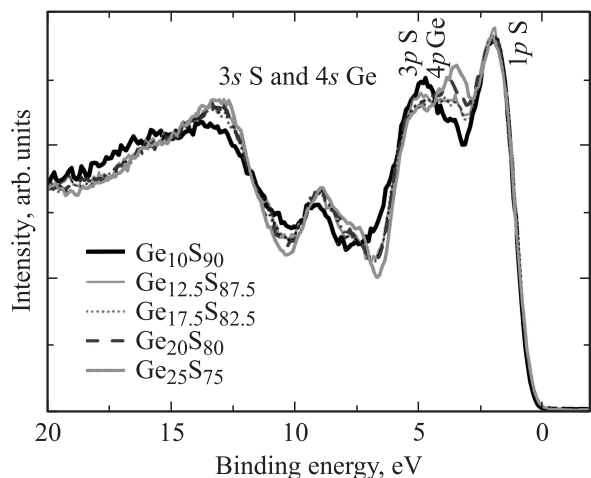


**Fig. 4.** Compositional behavior of XPS valence band spectra for  $\text{Ge}_x\text{S}_{100-x}$  glasses.

obtained for stoichiometric  $\text{GeSe}_2$  and  $\text{GeS}_2$  glasses [14,15]. The well-defined contributions from lone pair ( $1p$ ) electrons at about 2 eV, bonding states at about 5 eV and  $s$  electrons at 9–16 eV of chalcogen atoms are prominently visible in Figs 3 and 4 for chalcogen-rich  $\text{Ge}_x\text{Se}_{100-x}$  and  $\text{Ge}_x\text{S}_{100-x}$  ChVS samples. Increase in Ge concentration ( $x$ ) within the binary  $\text{Ge}_x\text{Se}_{100-x}$  and  $\text{Ge}_x\text{S}_{100-x}$  systems leads to a drop in the intensity of XPS signal from chalcogen  $1p$  electrons. The valley at  $\sim 3$  eV begins to fill and a density-of-states maximum develops due to the broadening of Se  $4p$  or S  $3p$  bonding states peak by the increased number of Se–Ge or S–Ge bonds [12–15]. An accompanying decrease in the band intensity at  $\sim 5$  eV is explained by a decrease in the density-of-states associated with chalcogen-chalcogen covalent bonds. Like in the case of As-based ChVS, full width at half maximum of the broad feature at 0–6 eV decreases with increasing of Ge content for

selenide samples, while analogous decrease for  $\text{Ge}_x\text{S}_{100-x}$  ChVS is margin.

Comparison of the compositional dependence of XPS valence band spectra obtained for  $\text{As}_x\text{Se}_{100-x}$  and  $\text{Ge}_x\text{Se}_{100-x}$  ChVS (Figs 1, 3) leads to a conclusion that in Se-rich ChVS  $4s$  states of Se contribute to the regions in valence band XPS spectra at  $\sim 11$  and  $\sim 16$  eV. In the case of sulfide glasses of  $\text{As}_x\text{S}_{100-x}$  and  $\text{Ge}_x\text{S}_{100-x}$  families (Figs 2, 4), the contribution from S  $3s$  states also can be seen around  $\sim 11$  and  $\sim 16$  eV, but these features are not so evident as in the case of selenide ChVS. With increasing  $x$ , the above two singularities originating from  $s$  states of chalcogen atoms, presumably, converge into a broad band near  $\sim 14$  eV for both selenide and sulfide ChVS. Owing to the compositional dependences of XPS valence band spectra for the investigated materials (Figs 1–4), the dominant input from As  $4s$  states is observed around  $\sim 9$  eV and from Ge  $4s$  states around  $\sim 8$  eV, which is in good agreement with theoretically predicted values [14,20].

Recently, it is shown that structure of chalcogen-rich arsenic-based ChVS obeys a so-called chain-crossing model [8,21]. This model can adequately describe the structure of  $\text{As}_x\text{Se}_{100-x}$  ChVS up to stoichiometric composition  $\text{As}_{40}\text{Se}_{60}$  [8], while it is less relevant for  $\text{As}_x\text{S}_{100-x}$  glasses [21]. For the latter ChVS even partitioning of covalent network is expected at  $x < 25$ , associated with detachment of  $\text{S}_8$  rings from the main glass backbone [16,22]. According to chain crossing model, the glass structure is built of As-based pyramids, which are homogeneously distributed in the glass-forming network and linked together by Se chains of approximately the same length. The average number of Se atoms within one chain between two As atoms depends only on ChVS composition (higher the chalcogen content, the longer would be the chalcogen-based chains). Therefore, with increase  $x$  the length of chalcogen chains, which interconnect pyramids, decreases being also the reason for the observed modifications in XPS valence band spectra of As-based ChVS.

In the case of Ge-based ChVS, the chain-crossing model describes atomic structure of chalcogen-rich glasses (within  $\sim 5$ –10% accuracy) only when  $x < 12$ . The outrigger raft scheme is more appropriate for network development in these materials [23]. It relies on the formation of structural fragments proper to high-temperature modifications of crystalline  $\text{GeSe}_2$  or  $\text{GeS}_2$  [23,24]. These fragments consist of two edge-shared tetrahedra connected with four corner-shared tetrahedra [24]. It was shown for selenide ChVS, that most of Ge atoms participated in the formation of structural units proper to high-temperature crystalline form of  $\text{GeSe}_2$  in all compositions starting from  $x = 20$  onward. So, the observed features in XPS valence band spectra of Ge-based ChVS reflect not only the shortening of chalcogen chains caused by decrease in chalcogen concentration, but also electronic signature of outrigger raft clustering in compositions with higher  $x$ .

## 4. Conclusions

Systematic variation of composition in  $\text{As}_x\text{Se}_{100-x}$ ,  $\text{As}_x\text{S}_{100-x}$ ,  $\text{Ge}_x\text{Se}_{100-x}$  and  $\text{Ge}_x\text{S}_{100-x}$  ChVS systems allows one to accomplish a more precise analysis and identification of XPS spectral features than from the data on any one composition. It is shown that observed composition dependences of the valence band electronic structure are dominated by chalcogen content in the investigated glasses, which distribution in the covalent-bonded networks of the investigated materials satisfies chain-crossing model in the case of As-based ChVS and outrigger raft scheme of network formation in the case of Ge-based glasses.

The authors acknowledge support from Russian–Ukrainian Projects No F28.2/076 and 09-03-90456 funded by State Fund for Fundamental Research in Ukraine and Russian Fund for Fundamental Research. R.G. thanks U.S. National Science Foundation, through International Materials Institute for New Functionality in Glass (IMI-NFG), for initiating the international collaboration and providing partial financial support for this work (NSF Grant No DMR-0409588).

## References

- [1] B.T. Kolomiets, N.A. Goryunova. *Zh. Tekh. Fiz.* **25**, 2069 (1955).
- [2] A. Feltz. *Amorphous Inorganic Materials and Glasses* (N.Y., VCH Publishers, 1993).
- [3] N.F. Mott, E.A. Davis. *Electron Processes in Non-Crystalline Materials* (Oxford, Clarendon Press, 1977).
- [4] J.S. Sanghera, I.D. Aggarwal. *J. Non-Cryst. Sol.*, **256–257**, 6 (1999).
- [5] B. Bureau, X.H. Zhang, F. Smektala, J.-L. Adam, J. Troles, H.-li Ma, C. Boussard-Plédel, J. Lucas, P. Lucas, D. Le Coq, M.R. Riley, J.H. Simmons. *J. Non-Cryst. Sol.*, **345&346**, 276 (2004).
- [6] A. Kovalskiy, M. Vlcek, J. Cech, W.R. Heffner, C.M. Waits, M. Dubey, H. Jain. *J. Micro/Nanolithography*, **8**(4), 043 012 (2009).
- [7] S.K. Sundaram, B.R. Johnson, M.J. Schweiger, J.E. Martinez, B.J. Riley, L.V. Saraf, N.C. Anheier, jr., P.J. Allen, J.F. Schultz. *Proc. SPIE*, **5359**, 234 (2004).
- [8] R. Golovchak, A. Kovalskiy, A.C. Miller, H. Jain, O. Shpotyuk. *Phys. Rev. B*, **76**, 125 208 (2007).
- [9] T. Takahashi, K. Murano, K. Nagata, Y. Miyamoto. *Phys. Rev. B* **28**, 4893 (1983).
- [10] H.A. Bullen, M.J. Dorko, J.K. Oman, S.G. Garret. *Surf. Sci.*, **531**, 319 (2003).
- [11] W. Li, S. Seal, C. Rivero, C. Lopez, K.A. Richardson, A. Pope, A. Schulte, S. Myneni, H. Jain, K. Antoine, A.C. Miller. *J. Appl. Phys.*, **98**, 053 503 (2005).
- [12] E. Bergignat, G. Hollinger, H. Chermette, P. Pertosa, D. Lohez, M. Lannoo, M. Bensoussan. *Phys. Rev. B*, **37**, 4506 (1988).
- [13] B.R. Orton, T. Punser, G. Malra, J.C. Riviere. *Structure of Non-Crystalline Materials* (Proceedings of the Second International Conference, 1983) p. 181.
- [14] S. Blaineau, P. Jund. *Phys. Rev. B*, **7**, 184 210 (2004).
- [15] K. Hachiya. *J. Non-Cryst. Sol.*, **312&314**, 566 (2002).

- [16] Z.U. Borisova. *Glassy Semiconductors* (N.Y., Plenum Press, 1981).
- [17] P. Krecmer, A.M. Moulin, R.J. Stephenson, T. Rayment, M.E. Welland, S.R. Elliott. *Science*, **277**, 1799 (1997).
- [18] R. Golovchak, A. Kozdras, O. Shpotyuk. *Sol. St. Commun.*, **145**, 423 (2008).
- [19] J.F. Moulder, W.F. Stickle, P.E. Sobol, K.D. Bomben. *Handbook of X-ray Photoelectron Spectroscopy*, ed. by J. Chastein (Perkin-Elmer Corp., Phys. Electron Div., Eden Prairie, Minnesota, 1992).
- [20] D.A. Drabold, J. Li, D.N. Tafen. *J. Phys.: Condens. Matter.*, **15**, S1529 (2003).
- [21] R. Golovchak, O. Shpotyuk, J.S. McCloy, B.J. Riley, C.F. Windisch, S.K. Sundaram, A. Kovalskiy, H. Jain. *Phil. Mag.* (2010) in press.
- [22] S. Tsuchihashi, Y. Kawamoto. *J. Non-Cryst. Sol.*, **5**, 286 (1971).
- [23] R. Golovchak, O. Shpotyuk, S. Kozyukhin, A. Kovalskiy, A.C. Miller, H. Jain. *J. Appl. Phys.*, **105**, 103 704 (2009).
- [24] J.E. Griffiths, G.P. Espinosa, J.C. Phillips, J.P. Remeika. *Phys. Rev. B*, **28**, 4444 (1983).

Редактор Т.А. Полянская